ANALYSIS ON THREE-DIMENSIONAL FLOW AND HEAT TRANSFER IN A CROSS WAVY PRIMARY SURFACE RECUPERATOR FOR A MICROTURBINE SYSTEM

by

Xiaohong GUI [a*], Xiange SONG [b], Tie LI [a], and Dawei TANG [a]

[a] Institute of Engineering Thermophysics, Chinese Academy of Sciences, Beijing, China
[b] Beijing International Studies University, Beijing, China

Original scientific paper
DOI: 10.2298/TSCI120410209X

In this paper, 3-D periodic numerical model for fully developed flow in a cross wavy primary surface recuperator for a microturbine system is built. The performance of flow and heat transfer is analyzed. The fields of flow and temperature in a gas and air channel are obtained. Different working conditions are numerically simulated. Numerical results are compared with experimental data concerned. Analysis results show that the flow in the gas and air channel is anti-symmetry along the centre of channel. The flow of fluid is fluctuant. The flow velocity of gas is much higher than that of air. The thermal ratio of cross wavy primary surface recuperator can reach 95.2%. The thermal ratio decreases with the improvement of gas inlet temperature. When gas inlet temperature increases by 100 K, the thermal ratio decreases by about 1%. The thermal ratio increases with the reduction of flow rate in the channel. When flow rate reduces by 40%, the thermal ratio increases by about 4%. The research results can be used to guide checking the performance of a recuperator.

Key words: *cross wavy primary surface recuperator, thermal ratio, periodic, numerical simulation*

Introduction

With the fast development of advanced manufacture technology, microturbines of high performance and low emissions which use multi fuel are about to find acceptance in large quantities in the distributed power generation field. For this type of microturbine generator of near 100 kW, an exhaust heat recovery recuperator is an absolutely necessary in order to realize a thermal efficiency of 30% or higher [1-3]. Besides the given requirement of compact size and high heat transfer area density, the performance of the recuperator will have direct influence on economical benefit or running cost of the whole system. The technology of recuperator is the pivotal technology in developing the microturbine generator device.

A microturbine system is made up of a centrifugal compressor, a centripetal turbine, a combust chamber, and a recuperator. The cross wavy primary surface recuperator (CWPSR) is a new recuperator concept that meets the demanding requirement for microturbines [4-6]. All of its heat transfer surfaces are all made up of thin stainless steel foils, and both sides contact di-

* Corresponding author; e-mail: guixiaohong@iet.cn

rectly with the cold and hot fluid, respectively. The hydraulic diameter of the flow channels is around 1 mm, which makes its heat transfer area density in excess of 1600 m^2/m^3. The corrugation of CWPSR influences the performance of flow and heat transfer directly. The flow in a channel is very complex. By numerical simulation, the performance of flow pattern and heat transfer in CWPSR can be better understood. The research results can be used to guide the designing and optimization for structure geometry and performance parameters.

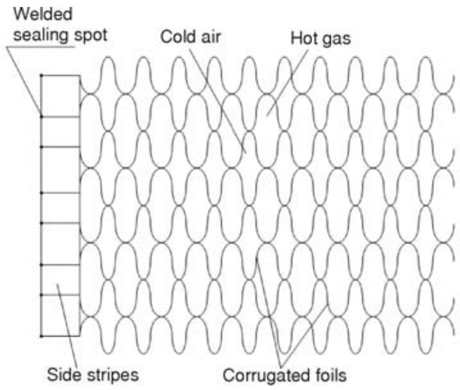

Figure 1. The cross-section of primary surface recuperator core

Structural characteristics and geometry model of a CWPSR for a microturbine system

The CWPSR is mainly composed of core, exhaust ducts and structure supporting assembly. The core is the main heat transfer part. It is the core that the whole recuperator depends on to realize the heat exchange between the flue gas of high temperature but low pressure from turbine and the air of low temperature but high pressure from compressor. The honeycomb core of CWPSR is made up of many stainless steel corrugated foils and side stripes arranged in turn and in order (fig. 1). The piled foils bring lots of small channels with hydraulic diameters around 1 mm. When the flue gas from microturbine and the air from compressor countercurrent flow through these channels formed by numerous corrugated foils, the heat transfer from the hot gas to the cold air through the solid corrugated foils is realized [7, 8] .

In this paper, a flow unit of CWPSR for a 100 kW microturbine is shown in fig. 2. It is stretched by a sine curve. The upper and lower plates of a generic couple share the same basic geometry. This CWPSR has a lot of design geometry parameters. It is characterized by corrugation plate geometry parameters as follows: pitch P, internal height H, wavelength λ, the height along the flow direction a, air side circle radius r, and gas side circle radius R. In the present study, the thickness of the plate is fixed as 0.1 mm, which could be commercially available. The description of key design parameters is shown in tab. 1.

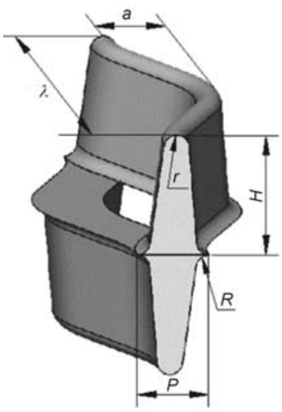

Figure 2. A flow unit

Table 1. Description of CWPSR key design parameters

Parameters	Value
Power, [kW]	100
Thermal ratio, [%]	88
Total pressure drop over recuperator, [%]	3
Pitch, [m]	0.0096
Internal height, [m]	0.001
Height in the flow direction, [m]	0.0011
Air side circle radius, [m]	0.00035
Gas side circle radius, [m]	0.00055

Numerical simulation of 3-D flow and heat transfer in cross wavy primary surface recuperator for a microturbine system

Physical model

The physical model of the air core unit is shown in fig. 3. The physical model of the gas core unit is shown in fig. 4. The gas and air channel are anti-symmetry.

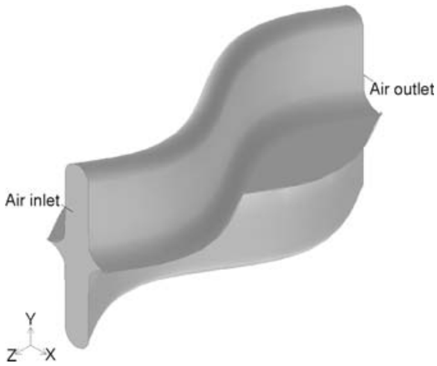

Figure 3. The physical model of the air core unit

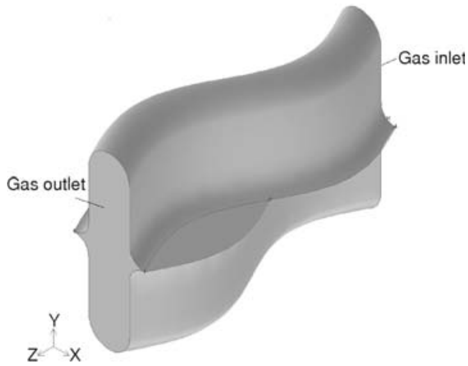

Figure 4. The physical model of the gas core unit

In order to simulate the periodic flow in the cross wavy primary surface, some assumptions are made.

The flow in the cross wavy primary surface is fully developed. In one flow unit, the velocity distribution form of inlet is the same with that of outlet, and there is a pressure drop between inlet and outlet. The flow and heat transfer in units are periodic, and one unit can represent the whole cross wavy primary surface core.

Mathematical model

The general equation of flow and heat transfer for 3-D steady variant physical property is defined as [9]:

$$\nabla(\rho\vec{V}\phi) = \nabla(\Gamma_\phi \nabla\phi) + S_\phi \tag{1}$$

– continuum equation

$$\phi = 1, \quad \Gamma_\phi = 0, \quad S_\phi = 0 \tag{2}$$

– momentum equation (ϕ is u, v and w)

$$\Gamma_\phi = \mu, \quad S_\mathrm{u} = \frac{-\partial p}{\partial x}, \quad S_\mathrm{v} = \frac{-\partial p}{\partial y}, \quad S_\mathrm{w} = \frac{-\partial p}{\partial z} \tag{3}$$

– energy equation

$$\phi = T, \quad \Gamma_\phi = \frac{\mu}{\mathrm{Pr}}, \quad S_\phi = 0 \tag{4}$$

The functions between thermal properties and temperature for working fluid (air and gas) are shown in tab. 2.

Table 2. Thermal properties of working fluid (air and gas)

Property	Air	Gas
Density [kgm^{-3}]	$\rho_a = 1.25363 - 0.00377\, t_a + 7.85868e{-}6\, t_a^2 - 9.27034e{-}9\, t_a^3 + 4.54004e{-}12\, t_a^4$	$\rho_g = 1.28457 - 0.00376\, t_g + 6.50294e{-}6\, t_g^2 - 5.51217e{-}9\, t_g^3 + 1.75065e{-}12\, t_g^4$
Specific heat capacity [Jkg^{-1}K^{-1}]	$C_{pa} = 920.96559 + 0.99151\, t_a - 0.0034\, t_a^2 + 6.2337e{-}6\, t_a^3 - 4.03812e{-}9\, t_a^4$	$C_{pg} = 1042.88914 + 0.22214\, t_g + 2.27831e - 4t_g^2 - 2.50154e{-}7\, t_g^3 + 6.45311e{-}11\, t_g^4$
Thermal conductivity [Wm^{-1}K^{-1}]	$k_a = 0.02548 + 6.2708e{-}5\, t_a + 6.14251e{-}8\, t_a^2 - 1.76779e{-}10\, t_a^3 + 1.1701e{-}13\, t_a^4$	$k_g = 0.02277 + 8.67973e{-}5\, t_g - 5.83513e{-}9\, t_g^2 + 8.50302e{-}12\, t_g^3 - 3.3851e{-}15\, t_g^4$
Viscosity [m^{2}s^{-1}]	$\mu_a = 3.00732e{-}5 - 1.10205e{-}7\, t_a + 9.20845e{-}10\, t_a^2 - 1.44589e{-}12\, t_a^3 + 8.77782e{-}16\, t_a^4$	$\mu_g = 1.17048e{-}5 + 8.79755e{-}8\, t_g + 9.075e{-}1\, t_g^2 - 1.64815e{-}14\, t_g^3 - 7.88861e{-}30\, t_g^4$

An approach to solution

Computational fluid dynamics software (FLUENT 6.2) is used to simulate the flow and heat transfer in a cross wavy primary surface. Software (GAMBIT 2.1) is used as a pre-processor. In FLUENT 6.2, the separate solver is used to solve the equations. Finite control volume method is used to solve the above equations. Thus, non-linear differential equations are linearized. Semi-implicit method for pressure-linked equation (SIMPLE) and alternate direction iteration method are used as a method of solution. The numerical model is defined as steady, laminar pressure-based model. The discretization methods for continuum equations, momentum equations and energy equations are defined as first order upwind.

Table 3. Key input data for CWPSR

Parameter	Value
Air inlet temperature, [K]	463
Gas inlet temperature, [K]	927
Air outlet temperature, [K]	873
Gas outlet temperature, [K]	529
Air flow rate, [kgs^{-1}]	0.998
Gas flow rate, [kgs^{-1}]	1.014
Thickness of solid wall, [m]	0.0001
Thermal conductivity of solid wall, [Wm^{-1}K^{-1}]	22.8

Boundary conditions

The inlet and outlet for both air and gas are defined as periodic boundary. The related mass flow, pressure gradient and upstream temperature are defined in detail. Other boundaries are defined as symmetry. The corresponding user defined functions are programmed. The key input data for CWPSR is shown in tab. 3.

Results and discussion

Analysis on the performance of flow and heat transfer in the recuperator

The flow field at air outlet is shown in fig. 5. The flow field at gas outlet is shown in fig. 6. As it can be seen, the flow in the gas and air channel is anti-symmetry along the centre of channel. The flow of fluid is fluctuant. The wavy flow strengthens the heat transfer greatly. The minimum velocity at air outlet is 6 m/s. The maximum velocity at air outlet is 16 m/s. The minimum velocity at gas outlet is 1 m/s. The maximum velocity at gas outlet is 5 m/s. So the velocity at air outlet is much higher than that at gas outlet. The reason is that the pressure at air inlet is much higher than that at gas inlet.

The temperature field distribution at the centre of the cross-section in the gas core unit (y = 0) is shown in fig. 7. The temperature field distribution at the centre of the cross-section in the gas core unit (x = 0) is shown in fig. 8. The temperature field distribution at the gas outlet is shown in fig. 9. The temperature field distribution at the air outlet is shown in fig. 10. The temperature field distribution at the centre of the cross-section in the air core unit (y = 0) is shown in fig. 11. The temperature field distribution at the centre of the cross-section in the air core unit (x = 0) is shown in fig. 12. The impact of swirl flow on the temperature distribution for heat transfer is depicted.

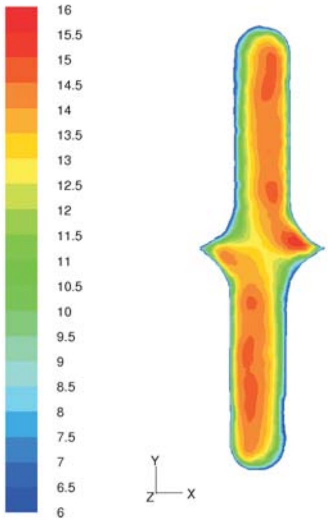

Figure 5. Flow field distribution at the air outlet [ms^{-1}]

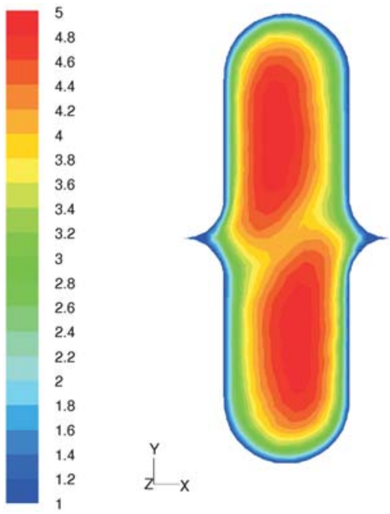

Figure 6. Flow field distribution at the gas outlet [ms^{-1}]

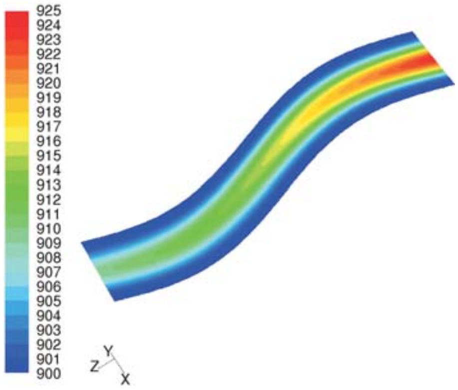

Figure 7. The temperature field distribution at the centre of the cross-section (y = 0) in the gas core unit [K]

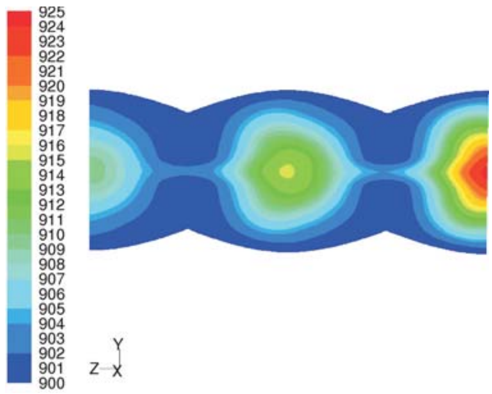

Figure 8. The temperature field distribution at the centre of the cross-section (x = 0) in the gas core unit [K]

As it can be seen, the thermal-hydraulic performance of the heat exchanger is strongly influenced by the surface-corrugation geometry of the plates employed in them. The enhanced heat transfer is directly related to these features, which provide increased effective heat transfer area, disruption, and re-attachment of boundary layers, swirl or vortex flow generation, and small hydraulic diameter flow channels. The temperature of gas decreases along the flow direction. The temperature at the gas inlet is higher than that at the gas outlet. The temperature of gas is higher than that on wall. Gas releases heat to wall by thermal conduction and convection. On

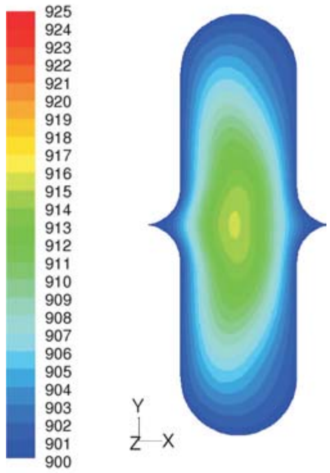

Figure 9. The temperature field distribution at the gas outlet [K]

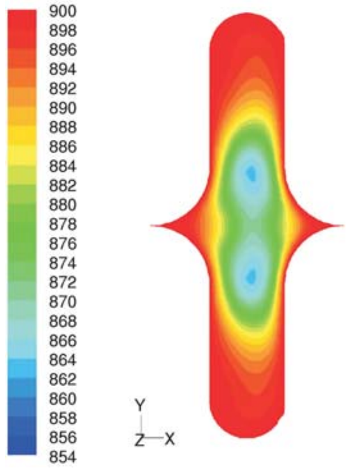

Figure 10. The temperature field distribution at the air outlet [K]

the contrary, the temperature of air increases along the flow direction. The temperature at the air inlet is lower than that of air outlet. The temperature of air is lower than that of wall. Air absorbs heat from wall by thermal conduction and convection.

Since the flow direction in gas channel is contrary to that in air channel, the thermal ratio ε is defined as:

$$\varepsilon = \frac{T_x - T_2}{T_1 - T_2} \qquad (5)$$

The thermal ratio is 95.2% by numerical simulation. Since the designing value is 88% (see tab. 1), the working condition of CWPSR satisfies original designing, and the thermal ratio of CWPSR is very high.

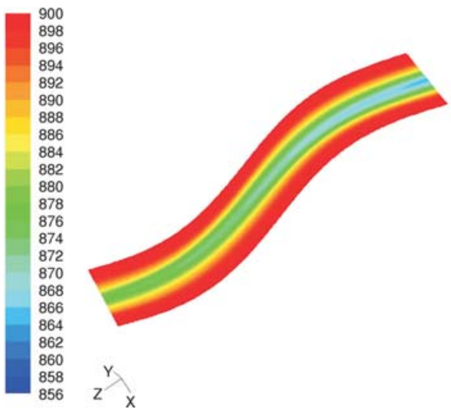

Figure 11. The temperature field distribution at the cross-section (y = 0) in the air core unit [K]

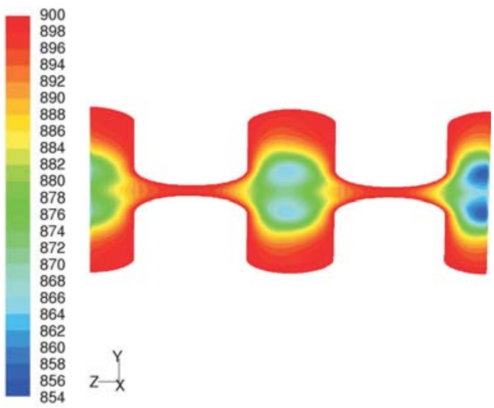

Figure 12. The temperature field distribution at the cross-section (x = 0) in the air core unit [K]

Influence of gas inlet temperature on thermal ratio and heat transfer rate

The comparison between our numerical results and experimental ones at Xi'an Jiaotong University [10] is shown in fig. 13. In the comparison, it can be seen that the corresponding differences of thermal ratio and heat transfer rate between our simulation and experiment at Xi'an Jiaotong University are small. The change trend of our numerical results agrees with experimental ones at Xi'an Jiaotong University. Therefore, our numerical results are credible. The heat transfer rate increases with gas inlet temperature. The thermal ratio decreases with the improvement of gas inlet temperature. The thermal ratio reduces by about 1% when gas inlet temperature increases by 100 K.

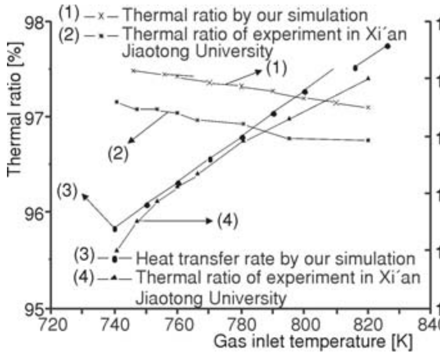

Figure 13. The comparison between our numerical results and experimental ones [10]

Influence of flow rate on thermal ratio and heat transfer rate

The recuperator working at different flow rate is simulated. The thermal ratio and heat transfer rate with flow rate are shown in fig. 14 when the flow rate of fluid reduces to 60%, 70%, 80%, and 90% of normal working condition. As it can be seen, the thermal ratio decreases with the improvement of flow rate. The thermal ratio increases by about 4% when the flow rate reduces by 40%. The research results are very important for checking the performance of the recuperator when microturbine works under partial workloads.

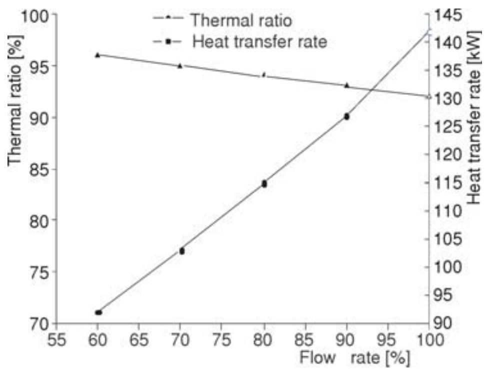

Figure 14. Influence of flow rate on the thermal ratio and heat transfer rate

Conclusions

3-D periodic numerical model for fully developed flow in a cross wavy primary surface recuperator for a microturbine system is built. The performance of flow and heat transfer is analyzed to better fit the special applications of interest. Numerical results are compared with experimental data concerned. Different simulations are successfully performed in order to assess the reliability of the results, in the operational range of interest for recuperated microturbine applications. The performance of the recuperator will have direct influence on economical benefit or running cost of the whole system. The technology of recuperator is the pivotal technology in developing the microturbine generator device. This paper reports the successful outcome of a comprehensive and predictive study of the problem of understanding the complex local flow and heat transfer patterns in the crossed wavy geometry. Some of the results obtained can be summarized as follows.

- The flow in the gas and air channel is anti-symmetry along the centre of channel. The flow of fluid is fluctuant. The flow velocity of air is much higher than that of gas. The wavy flow strengthens the heat transfer greatly.
- The thermal-hydraulic performance of the heat exchanger is strongly influenced by the surface-corrugation geometry of the plates employed in them. The enhanced heat transfer is directly related to these features, which provide increased effective heat transfer area, disruption, and re-attachment of boundary layers, swirl or vortex flow generation, and small hydraulic diameter flow channels.
- The thermal ratio of cross wavy primary surface recuperator is very high. The thermal ratio can reach 95.2%.
- The thermal ratio decreases with the improvement of gas inlet temperature. When gas inlet temperature increases by 100 K, the thermal ratio decreases by about 1%.

- The thermal ratio increases with the reduction of flow rate in the channel. When flow rate reduces by 40%, the thermal ratio increases by about 4%. The research results can be used to guide the designing and optimization for structure geometry and performance parameters.

Acknowledgments

The authors acknowledge the financial support provided by National Basic Research Program of China (Grant No.2012CB933200) and National Natural Science Foundation of China (Grant No.51476172).

Nomenclature

a	– height along the flow direction, [m]
C	– specific heat capacity, [$\mathrm{Jkg^{-1}K^{-1}}$]
H	– internal height, [m]
k	– thermal conductivity, [$\mathrm{Wm^{-1}K^{-1}}$]
P	– pitch, [m]
Pr	– Prandtl number, [–]
p	– pressure, [Pa]
R	– gas side circle radius, [m]
r	– air side circle radius, [m]
S	– source terms, [–]
T	– temperature,[K]
t	– temperature, [°C]
u	– velocity in x-direction, [$\mathrm{ms^{-1}}$]
v	– velocity in y-direction, [$\mathrm{ms^{-1}}$]
w	– velocity in z-direction, [$\mathrm{ms^{-1}}$]

Greek symbols

ε	– thermal ratio, [–]
λ	– wavelength, [m]
μ	– kinematic viscosity, [$\mathrm{m^2s^{-1}}$]
ρ	– density, [$\mathrm{kgm^{-3}}$]

Subscripts

a	– air
g	– gas
pa	– air at constant pressure
pg	– gas at constant pressure
x	– air outlet
1	– gas inlet
2	– air inlet

References

[1] Utriainen, E., Sunden, B., A Numerical Investigation of Primary Surface Rounded Cross Wavy Ducts, *Heat and Mass Transfer, 38* (2002), 7-8, pp. 537-542
[2] Wang, Q. W. *et al*., Genetic Algorithm Optimization for Primary Surfaces Recuperator of Microturbine, *Journal of Engineering for Gas Turbines and Power, 129* (2007), 4, pp. 436-442
[3] Zhang, H. Z., *et al*., Micro-Turbine Technology Is Developing, *Power Engineering, 21* (2001), 6, pp. 1532-1538
[4] McDonald, C. F., Heat Recovery Exchanger Technology for Very Small Gas Turbines, *Journal of Turbo and Jet Engines, 13* (1996), 4, pp.239-261
[5] McDonald, C. F., Low-Cost Compact Primary Surface Recuperator Concept for Microturbines, *Applied Thermal Engineering, 20* (2000), 5, pp. 471-497
[6] McDonald, C.F., Recuperator Considerations for Future Higher Efficiency Microturbines, *Applied Thermal Engineering, 23* (2003), 12, pp. 1463-1487
[7] Liu, Z. Y., Cheng, H. E., Multi-Objective Optimization Design Analysis of Primary Surface Recuperator for Microturbines, *Applied Thermal Engineering, 28* (2008), 4, pp. 601-610
[8] Ward, M. E., Holman, L., Primary Surface Recuperator for High Performance Prime Movers, *SAE Technical Paper Series, 15* (1992), 2, pp. 24-28
[9] Tao, W. Q., *Numerical Heat Transfer*, 2nd ed., Publishing House of Xi'an Jiaotong University, Xi'an, China, 2001
[10] Liang, H. X., *et al.*, Experimental Investigation of Flow and Heat Transfer in a Primary Surface Recuperator, *Journal of Engineering Thermophysics, 30* (2009), 12, pp. 2110-2112

Paper submitted: April 10, 2012
Paper revised: September 7, 2012
Paper accepted: November 20, 2012